

# Measurement of the $e^+e^- \rightarrow \pi^+\pi^-$ Cross Section in the Energy Range between $\rho$ and $\Phi$ Mesons

G.V.FEDOTOVICH\*

*Budker Institute of Nuclear Physics, Novosibirsk, 630090, Russia*

## ABSTRACT

The general purpose CMD-2 detector at the VEPP-2M collider in Novosibirsk has collected the luminosity integral of  $\sim 300 \text{ nb}^{-1}$  in the energy range between  $\rho$  and  $\Phi$  mesons. High accuracy measurements of the  $e^+e^-$  annihilation cross section in this energy region are required for the muon g-2 experiment at Brookhaven. The data are also important to interpret the fundamental Standard Model parameters known with high accuracy. Preliminary results of data analysis are presented.

## 1 - Introduction

The data on the cross section  $e^+e^- \rightarrow \pi^+\pi^-$  in the energy range between  $\rho$  and  $\Phi$  mesons were obtained with the CMD-2 detector <sup>1, 2)</sup> at the VEPP-2M collider <sup>3)</sup> at Budker Institute of Nuclear Physics in Novosibirsk. The data from the low energy region up to 1400 MeV (maximum energy provided by VEPP-2M) are important both for the search of rare decays of the light vector mesons and for the calculation

---

<sup>1</sup>CMD-2 collaboration:

R.R.Akhmetshin, G.A.Aksenov, E.V.Anashkin, V.M.Aulchenko, B.O.Baibusinov, V.S.Banzarov, L.M.Barkov, S.E.Baru, A.E.Bondar, D.V.Chernyak, V.V.Danilov, S.I.Eidelman, G.V.Fedotov, N.I.Gabyshev, A.A.Grebeniuk, D.N.Grigoriev, P.M.Ivanov, B.I.Khazin, I.A.Koop, A.S.Kuzmin, I.B.Logashenko, A.P.Lysenko, A.V.Maksimov, Yu.I.Merzlyakov, V.A.Monich, I.N.Nesterenko, V.S.Okhapkin, E.A.Perevedentsev, A.A.Polunin, E.V.Popkov, E.G.Pozdeev, V.I.Ptitzyn, T.A.Purlatz, S.I.Redin, N.I.Root, A.A.Ruban, N.M.Ryskulov, Yu.M.Shatunov, A.E.Sher, M.A.Shubin, B.A.Shwartz, V.A.Sidorov, A.N.Skrinsky, V.P.Smakhtin, I.G.Snopkov, E.P.Solodov, A.I.Sukhanov, V.M.Titov, Yu.V.Yudin, V.G.Zavarzin, S.G.Zverev - *Budker Institute of Nuclear Physics, Novosibirsk, Russia*; D.H.Brown, J.P.Miller, B.L.Roberts, W.A.Worstell - *Boston University, USA*; J.A.Thompson, C.Valine - *University of Pittsburgh, USA*; S.Dhawan, V.Hughes *Yale University, USA*; P.Cushman *University of Minnesota, USA*

of the dispersion integral that relates the cross section of  $e^+e^-$  annihilation into hadrons to the value of the hadronic vacuum polarization. This value plays an important role in the interpretation of the fundamental Standard Model parameters and the evaluation of the anomalous magnetic moment of the muon <sup>4, 5</sup>), which will be measured in the E821 experiment at BNL with an extremely high precision of 0.35 ppm. To evaluate the contribution of the hadronic vacuum polarization to the muon  $g-2$  with the same accuracy a systematic error in hadronic cross section should be less than 0.5%, because the value of the total hadronic contribution is equal to  $72 \pm 1.6$  ppm <sup>6</sup>). The main part of this contribution comes from the energy range which is provided by the VEPP-2M collider.

## 2 - Data Analysis

The data discussed in this talk were obtained by scanning the energy region between  $\phi$  and  $\rho$  mesons with 10 MeV step. About  $10^3$  of pion pairs were sampled at every point. The main part of the luminosity integral  $\sim 300 \text{ nb}^{-1}$  was collected during 1994 runs. Using the resonance depolarization technique <sup>7</sup>), the beam energy at each point was measured with the accuracy of  $10^{-4}$ . The detector trigger is described in <sup>8</sup>). Events were recorded when:

- \* at least one track in the Drift Chamber was found by the tracking processor <sup>9</sup>)
- \* the energy deposition in the CsI calorimeter was greater than 20 MeV.

About 20 million events were written on the magnetic tape. For off-line analysis only collinear two track events were selected. The cuts used for this selection are marked by arrows in Fig.1. Events were used in a maximum likelihood function fit with the following global optimization parameters:

- \* number of electrons  $N_e$
- \* number of background events  $N_b$
- \*  $\frac{N_\pi}{N_e + N_\mu}$ , where  $N_\pi$  - number of pions and  $N_\mu$  - number of muons.

The ratio  $N_\mu/N_e$  was fixed from the QED. The likelihood fit used information on the polar angle, longitudinal coordinate of the vertex and energies deposited in the CsI calorimeter. As it is seen from Fig.2 the experimental data are in a good agreement with the fit.

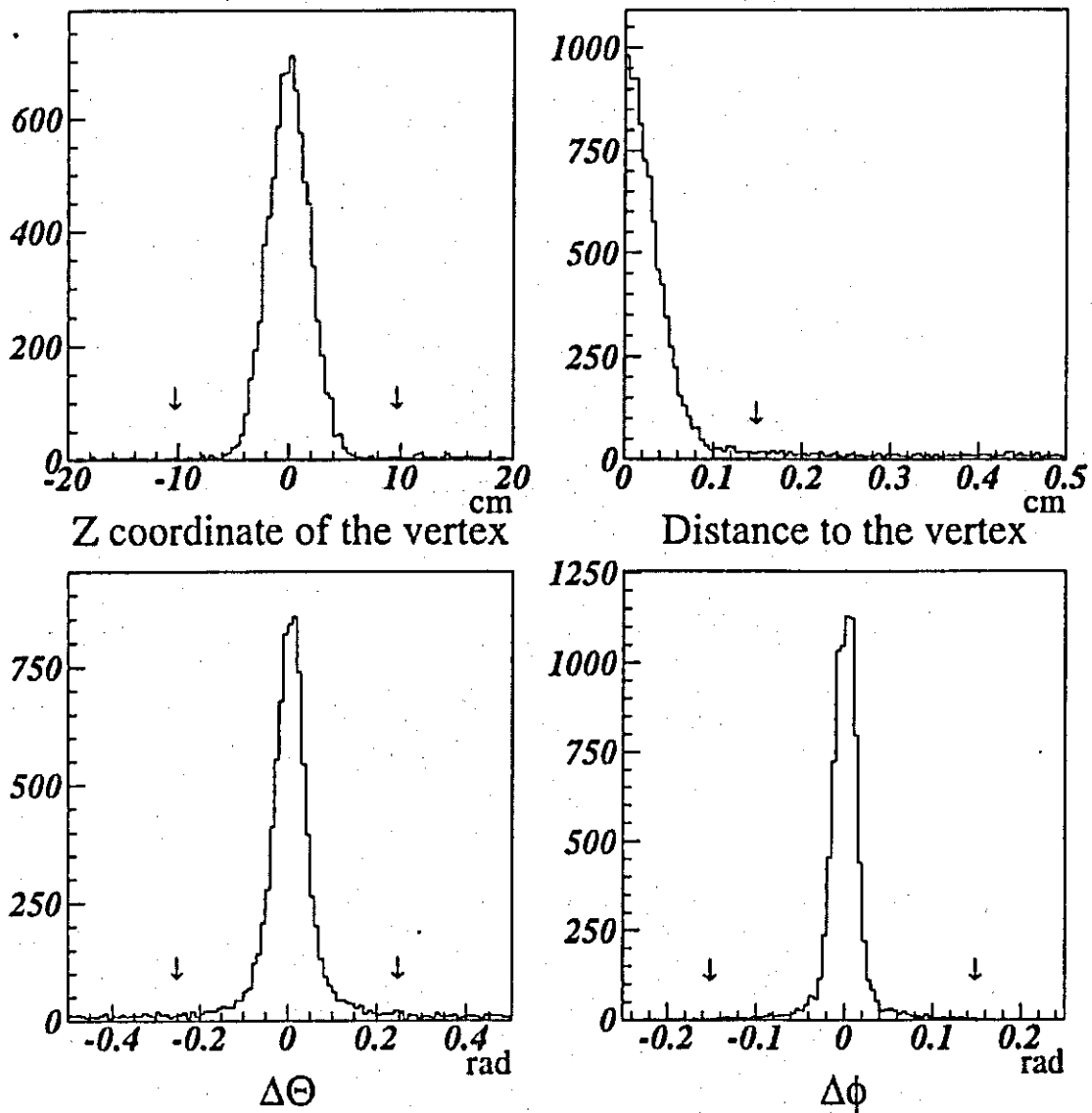


Figure 1: Two track events distributions and cuts imposed to select collinear events.

The ratio  $\frac{N_\pi}{N_e + N_\mu}$  allows to express  $e^+e^- \rightarrow \pi^+\pi^-$  cross section in a simple way:

$$\sigma_\pi = \frac{N_\pi}{N_e + N_\mu} \cdot \frac{\epsilon_e \sigma_e (1 + \delta_e) + \epsilon_\mu \sigma_\mu (1 + \delta_\mu)}{\epsilon_\pi (1 + \delta_\pi)}$$

where  $\epsilon_e, \sigma_e, \delta_e, \epsilon_\mu, \sigma_\mu, \delta_\mu, \epsilon_\pi, \sigma_\pi, \delta_\pi$  are detection efficiencies, cross sections and radiative corrections for electrons, muons and pions respectively. Pion formfactor values are presented in Fig.3 along with the results of the previous experiments.

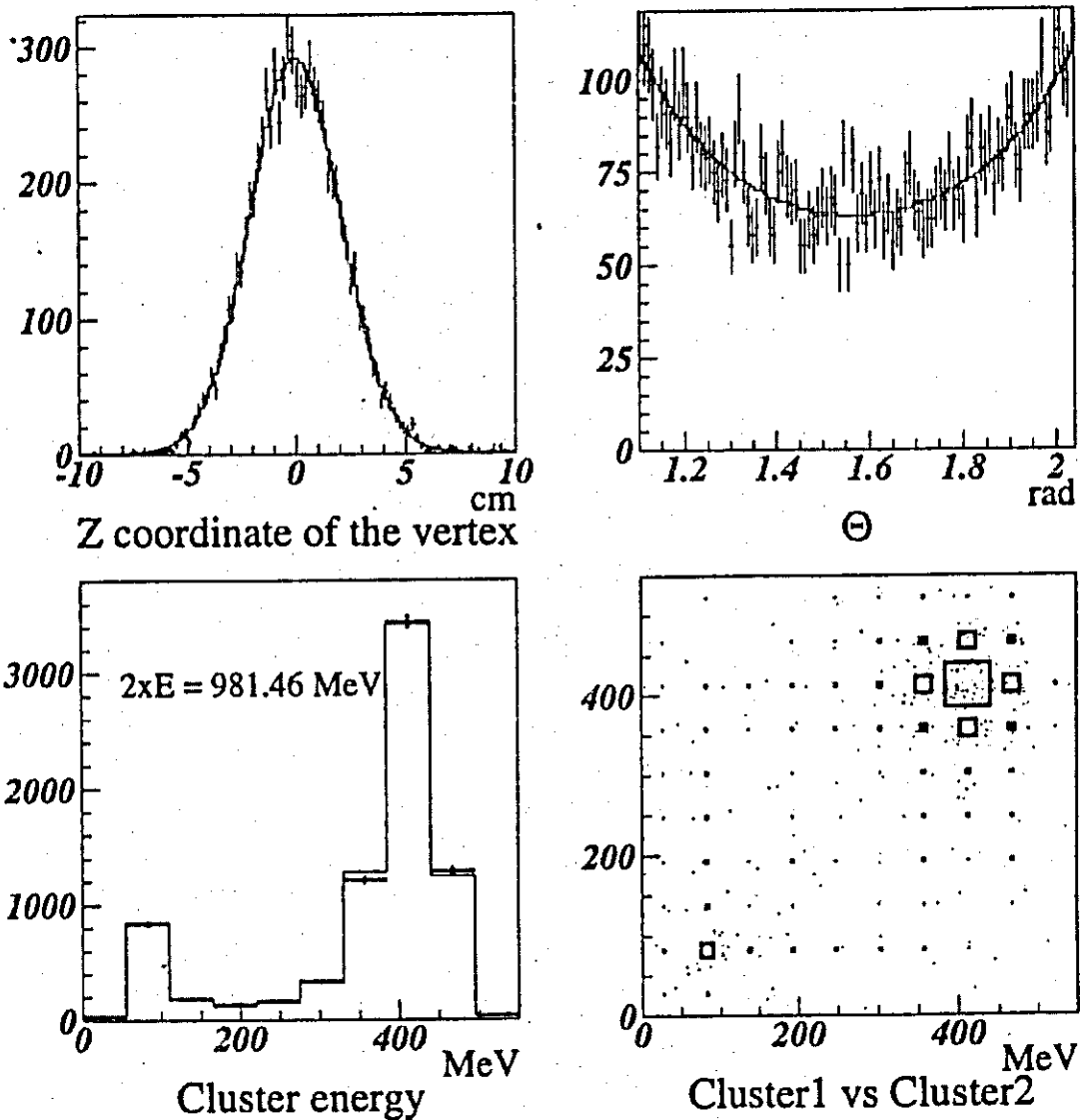


Figure 2: The comparison of the experimental data with a fit.

The statistical error of the  $\pi^+\pi^-$  cross section at each energy point is better than 3%. At present the total systematic error is estimated to be  $\sim 1.5\%$ . The main part of this error comes from the detector solid angle uncertainty  $\sim 1\%$  and from the calculation of the radiative corrections for Bhabha events <sup>10)</sup>, which are known with accuracy  $\sim 1\%$ . Radiative corrections for all other channels of the  $e^+e^-$  annihilation into hadrons and muons were calculated with the accuracy about 0.2 - 0.5% <sup>11, 12)</sup> which is sufficient for the purposes of the experiment. As an example, we describe very briefly the main idea and approach to calculation of the radiative corrections for the channel  $e^+e^- \rightarrow \pi^+\pi^-$  in Appendix.

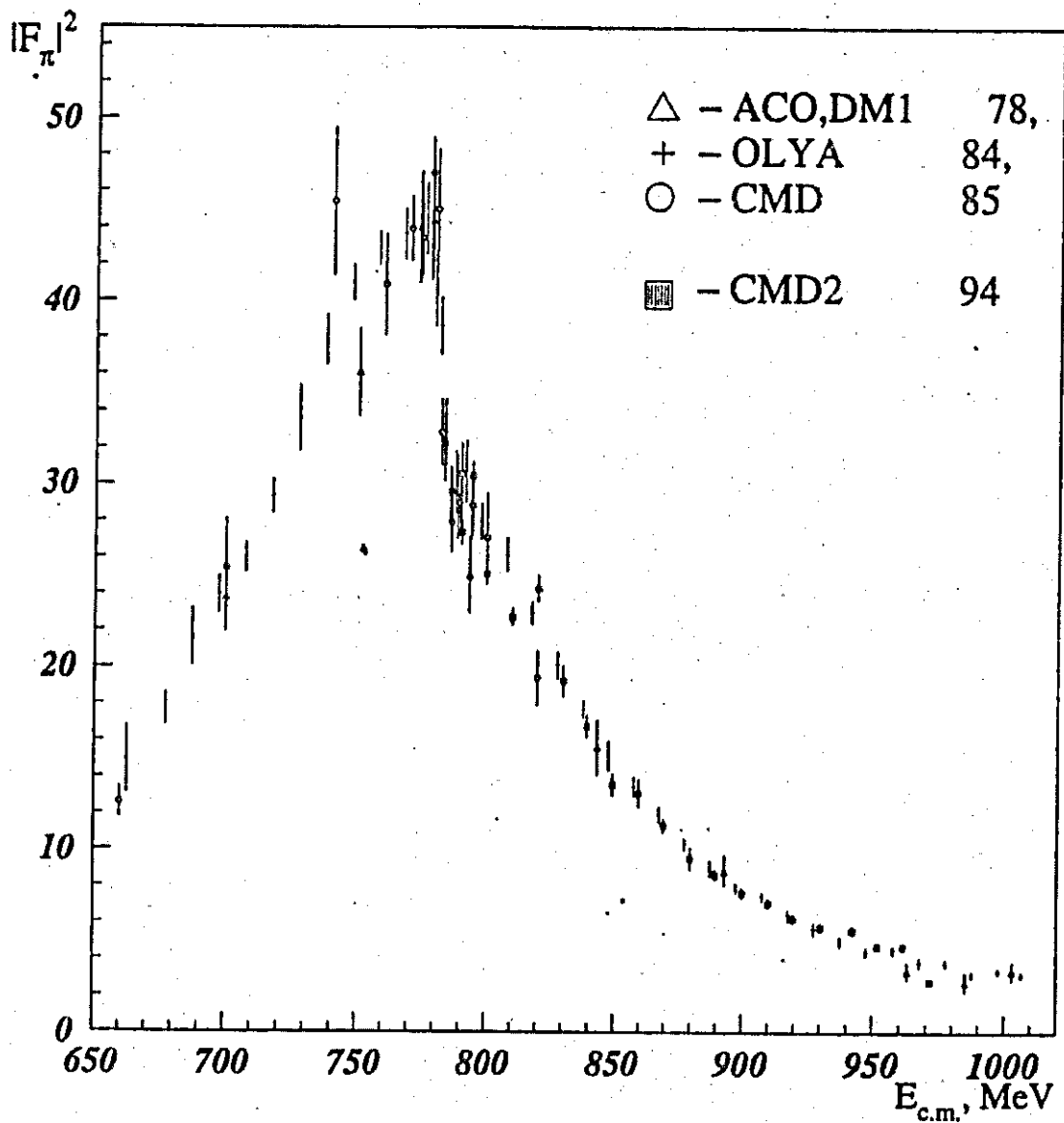


Figure 3: The experimental data for  $|F_\pi|^2$ .

The further improvement of the Drift Chamber parameters and more accurate calculations of the radiative corrections for Bhabha scattering events would decrease the systematic error to the level of 0.5%.

This work is supported in part by the US Department of Energy, US National Science Foundation and the International Science Foundation under the grant RPT000.

## References

1. G.A. Aksenov et al., Preprint INP 85-118, (Novosibirsk 1985).

2. B.I. Khazin et al., Proc. of the XXVI Int. Conf. on High Energy Physics, 2, 1876,(1992) (Ed. J.R. Sanford).
3. V.V. Anashin et al., Preprint INP 84-114, (Novosibirsk 1984).
4. M. Vysotski, Plenary talk, Proc. of the XXVII Int. Conf. on High Energy Physics.
5. Muon g-2 Design Report AGS 821, BNL, July (1992).
6. S. Eidelman and F. Jegerlehner, Preprint PSI-PR 95-01, (1995).
7. Ya.S. Derbenev et al., Part. Acc. 10, 177 (1980).
8. E.V. Anashkin et al., Nucl. Instr. Meth. A323, 178 (1992).
9. V.M. Aulchenko et al., Nucl. Instr. and Meth., A252, 299, (1986).
10. F.A. Berends and R. Kleiss, Nucl. Ph., B228, 537 (1983).
11. E.A. Kuraev, V.S. Fadin, Soviet Journal of Nuclear Physics, 41, 466, (1985).
12. E.A. Kuraev et al. Will be published.
13. F.A. Berends and G.J. Komen, Physics Letters, B63, 432, (1976).

### 3 -Appendix

Our technique for the calculation of the radiative corrections is based primarily on two works <sup>11, 12</sup>). The first one gives an accuracy about 0.2% but the cross section is integrated over all final particles kinematics except for the total energy loss and furthermore is valid only for comparatively small energy losses (under 10% of the beam energy). The second one is less accurate (about 0.5% ) and assumes that only one photon is emitted but it gives the angle distributions for the final particles, which is important when any selection criteria are applied to the events.

Our procedure for the calculation of the radiative corrections is combined both approaches in the following way: photons with the energy less than  $\Delta E$  are simulated according to <sup>11</sup>) while photons with the energy greater than  $\Delta E$  are simulated according to <sup>12</sup>). The quantity  $\Delta E$  is a free parameter and its selection will be discussed later. In order to get a smooth and continuous distributions over final particles kinematics, energy loss for a region under  $\Delta E$  was assigned to a "hypothetical" single photon having the same angular distributions as follows from <sup>12</sup>). The dependence of the radiative corrections for the channel  $e^+e^- \rightarrow \pi^+\pi^-$  on

the value of  $\Delta E$  is shown in Fig.4 under selection criteria (mentioned above in the talk) for the collinear events.

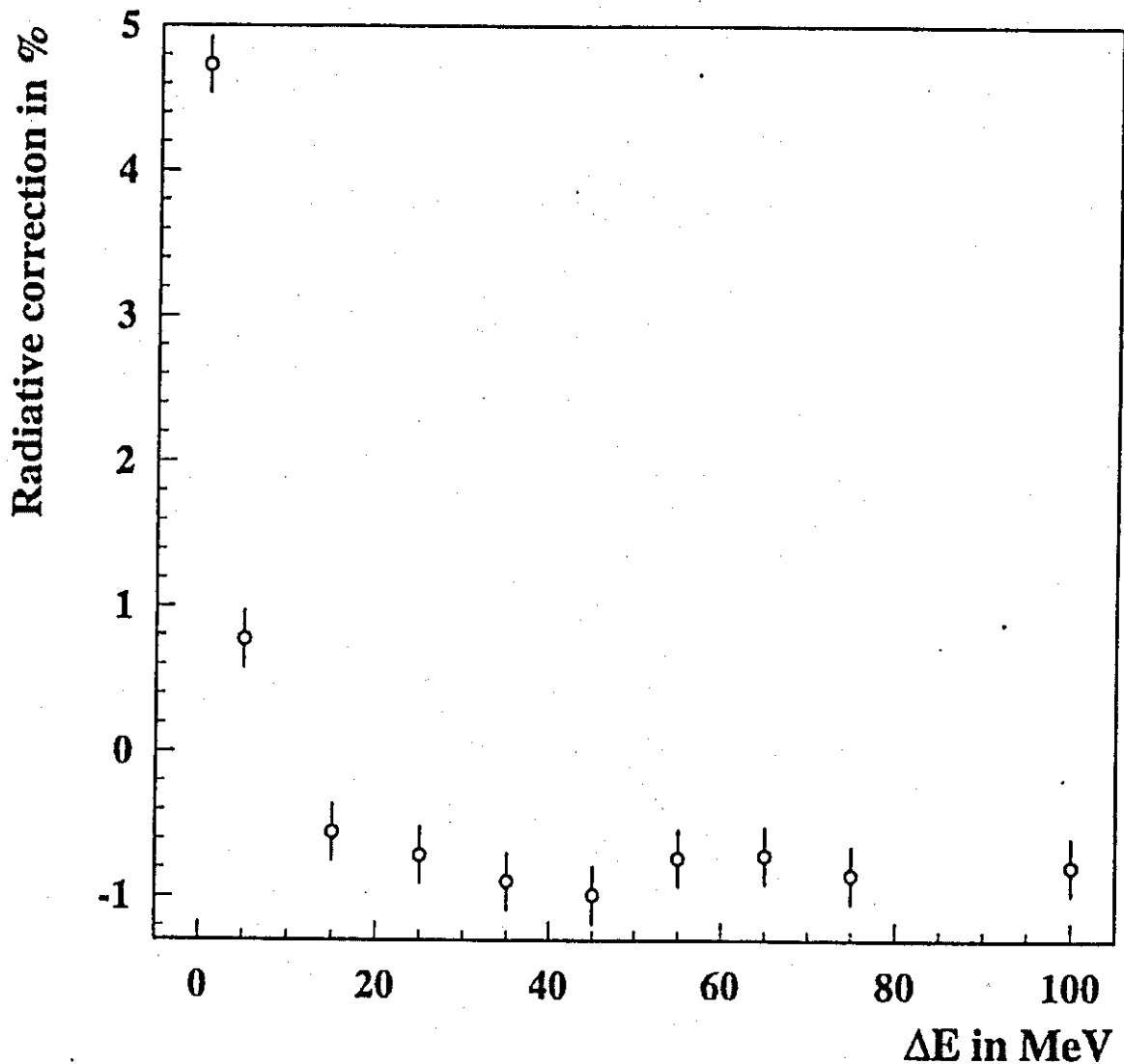


Figure 4: The dependence of the radiative corrections on  $\Delta E$  for the energy 952 MeV.

One can see that in a wide region of the  $\Delta E$  values the total cross section does not depend on  $\Delta E$  with the accuracy of about 0.2 – 0.3%.

The possible values of  $\Delta E$  are limited by the following factors:

- \*  $\Delta E$  should not exceed the validity region of <sup>11)</sup>
- \*  $\Delta E$  should be large enough for the approach of the single photon to be applicable
- \* it is desirable to have  $\Delta E$  as large as possible to use the

better accuracy of <sup>11)</sup>

\* for large energy losses causing the events rejecting by the selection criteria an approach <sup>12)</sup> should be used to take proper account of the final particles kinematic.

Thus the reasonable values of  $\Delta E$  are limited on both sides and should be somewhere from 20 to 50 MeV depending on the beam energy and the selection criteria of the collinear events.

The expression for the calculation of the radiative corrections for the channel  $e^+e^- \rightarrow \pi^+\pi^-$  is briefly described below. Calculations of the radiative corrections for the other channels were done in a similar way.

The cross section used for the calculation of the radiative corrections can be expressed as follow:

$$\frac{d\sigma_\pi(S)}{d\Omega_-} = \int_0^\Delta \frac{d\sigma_0(S_1)}{d\Omega_-} \cdot \frac{F(S, x_\gamma)}{|1 - \Pi(S_1)|^2} dx_\gamma +$$

$$+ \frac{2\alpha}{\pi} \int_\Delta^{x_\gamma \max} f_{en}(x_\gamma) dx_\gamma \int_{-1}^1 f_{ang}(Z_\gamma) dZ_\gamma \frac{d\sigma_0(S_1)}{d\Omega_-} \left| \frac{F_\pi(S_1)}{F_\pi^{BW}(S_1)} \right|^2 \frac{R(S, Z_-, x_\gamma, Z_\gamma)}{|1 - \Pi(S_1)|^2},$$

where

$$\frac{d\sigma_0(S)}{d\Omega_-} = \frac{\alpha^2}{8S} \beta_\pi^3 (1 - Z_-^2)$$

- is the Born cross section,

$$f_{en}(x_\gamma) = \frac{1}{x_\gamma(1-x_\gamma) \left[ \left(1 - \frac{S(1-x_\gamma)}{M_\rho^2}\right)^2 + \frac{\Gamma_\rho^2}{M_\rho^2} \right]}$$

- is a function used for the simulation of the photon energy,

$$f_{ang}(Z_\gamma) = \frac{1}{1 - \beta_e^2 Z_\gamma^2} \left[ 1 - \frac{1}{1 + \gamma_e^2 (1 - Z_\gamma^2)} \right]$$

- is a function used for the simulation of the polar angle of the photon emitted by the initial particles,

$|F_\pi(S)|^2$  - is the pion formfactor squared,

$|F_\pi^{BW}(S)|^2$  - is the pion formfactor squared in the simplest Breit-Wigner form,

$\Pi(S)$  - is the vacuum polarization due to leptons and hadrons <sup>11, 13)</sup>,

$F(S, x_\gamma)$  - is the structure function <sup>11)</sup>,

$$R(S, Z_-, x_\gamma, Z_\gamma) = \frac{1}{|1 - \Pi(S_1)|^2} \cdot \frac{1}{\beta_\pi^3 (1 - Z_-^2)} \cdot \left[ \frac{\beta_- x_-}{2 - x_\gamma (1 - \cos(\Phi)/\beta_-)} \right] \cdot |M|^2.$$



The expression in the squared brackets is connected with the phase space of the final particles.  $|M|^2$  is the dimensionless square of the matrix element for  $e^+e^- \rightarrow \pi^+\pi^-$  process from which the main peculiarities ( $f_{en}(x_\gamma)$  and  $f_{ang}(Z_\gamma)$ ) are factored out.

$$|M|^2 = \left[1 + \frac{1}{\gamma_e^2(1 - Z_\gamma^2)}\right] \cdot \frac{R_1 + R_2}{1 - x_\gamma},$$

where 12)

$$R_1 = [(2 - x_\gamma)^2 + x_\gamma^2 Z_\gamma^2](\beta_\pi^2 - x_\gamma) - (1 - x_\gamma)[(x_+ - x_-)^2 + (x_+ \beta_+ Z_+ - x_- \beta_- Z_-)^2]$$

and

$$R_2 = -\frac{1}{1 + \gamma_e^2(1 - Z_\gamma^2)} [4(1 - x_\gamma)(\beta_\pi^2 - x_\gamma) - (x_+(Z_\gamma + \beta_+ Z_+) - x_-(Z_\gamma + \beta_- Z_-))^2]$$

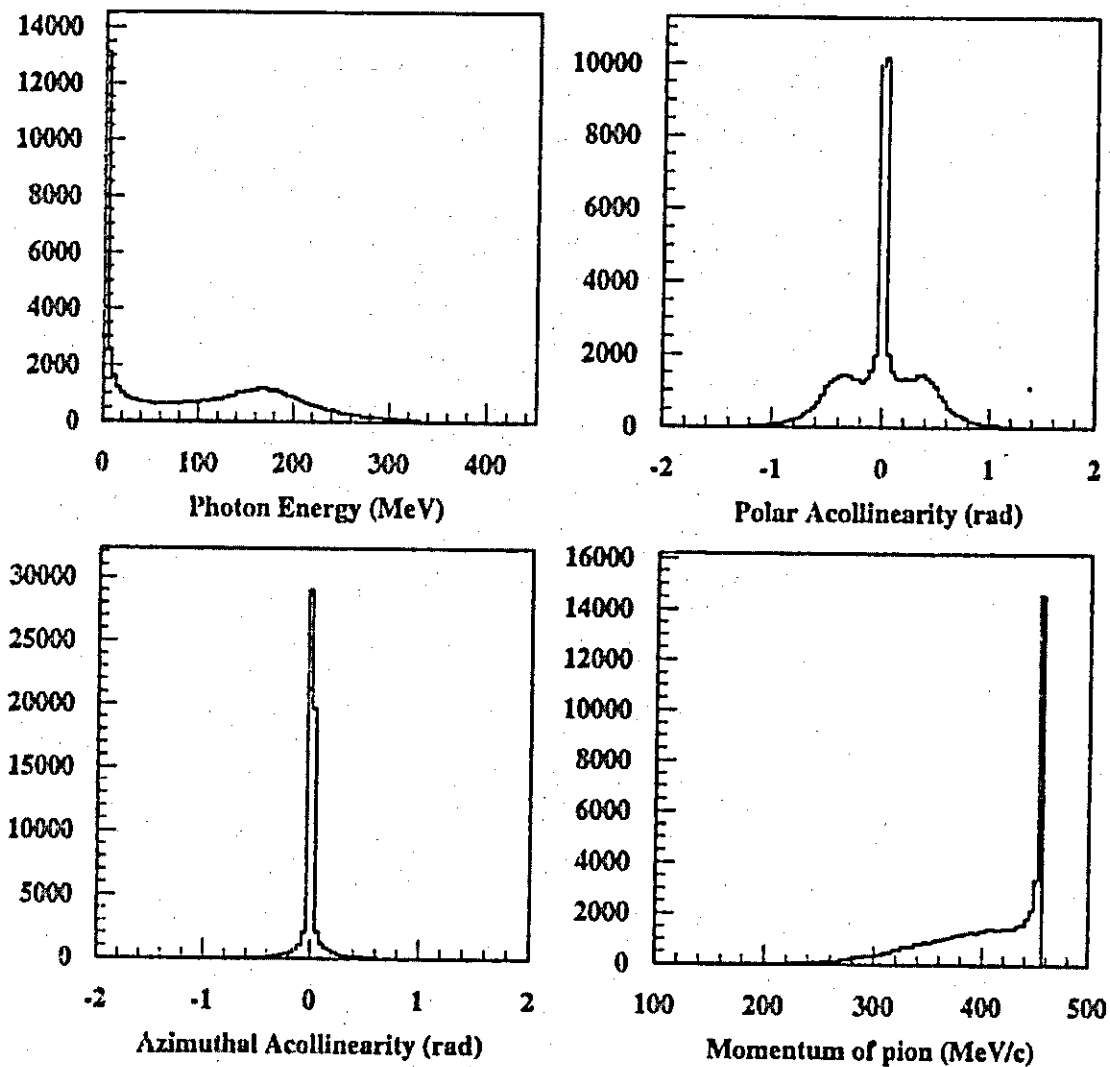


Figure 5: The distributions of the final state particles for the energy 952 MeV.

The following designations were used in the previous expressions:  $x_+$ ,  $x_-$ ,  $x_\gamma$  - energies of the final pions and photon divided by  $E_{beam}$  respectively;  $Z_-$ ,  $Z_+$ ,  $Z_\gamma$  - their polar angles cosines;  $\beta_+$ ,  $\beta_-$  - velocities of pions;  $S = 4E_{beam}^2$ ;  $S_1 = S(1-x_\gamma)$ ;  $\Delta = \Delta E/E_{beam}$ ;  $\gamma_e = E_{beam}/m_e$ ;  $\beta_e = P_e/E_{beam}$ ;  $\beta_\pi = P_\pi/E_{beam}$ ;  $E_{beam}$  - energy of the electron (positron);  $P_e$  - their momenta;  $m_e$  and  $m_\pi$  are the electron and pion masses.

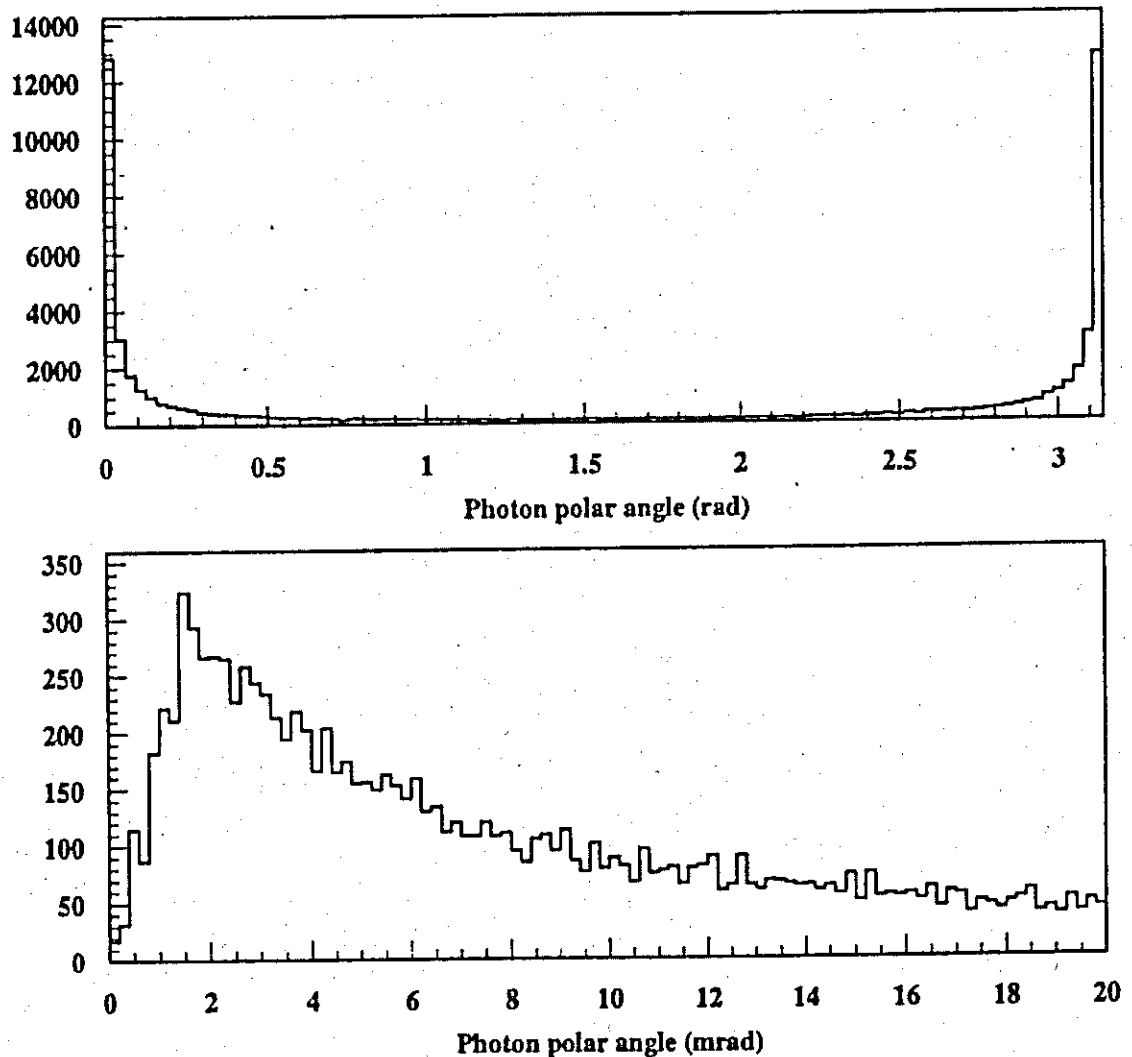


Figure 6: The photons distributions on the polar angle.

The  $|M|^2$  is a smooth function that provides a high efficiency of the simulation. For the photons with the energies less than  $\Delta E$  the efficiency is about 70-80% depending on the c.m.s. energy. For the photons with the energies more than  $\Delta E$  the efficiency varies from 10 to 60% depending on the c.m.s. energy, reaction channel and selection criteria.

According to expressions described above 50000 events of the  $e^+e^- \rightarrow \pi^+\pi^-\gamma$  process were simulated at the center of mass energy 952 MeV. Some of the distributions for the final state particles are shown in Fig.5-6. No selection criteria were used except that one of the charged particles should have the angles inside of the solid angle CMD-2 detector. On the first histogram of Fig.5 the energy spectrum of the emitted photons is represented. There is a bump near 160 MeV that corresponds to the dumping to  $\rho$  meson resonance. On the second histogram the polar acollinearity between two pions is shown. There are two symmetric bumps around the central peak that also correspond to the dumping to the resonance. On the third histogram the acollinearity between two pions in the azimuthal plane is shown. On the last histogram the momentum spectrum of pions is represented. The long tail can be explained by the emitted hard photons and by the dumping to the resonance. In Fig.6 two distributions over polar angles of the emitted photons are represented. The last one shows a small polar angles region in more details.